When are antiaromatic molecules paramagnetic?

Rashid R. Valiev,[a,b,*] Glib V. Baryshnikov,[c,d,*] Rinat T. Nasibullin,[e] Dage Sundholm,[b] and Hans Ågren[f,c]

[a] *Research School of Chemistry & Applied Biomedical Sciences, National Research Tomsk Polytechnic University, Lenin Avenue 30, Tomsk 634050, Russia*

[b] *Department of Chemistry, Faculty of Science, University of Helsinki, FIN-00014, Helsinki, Finland*

[c] *Division of Theoretical Chemistry and Biology, School of Engineering Sciences in Chemistry, Biotechnology and Health, KTH Royal Institute of Technology, 10691, Stockholm, Sweden*

[d] *Department of Chemistry and Nanomaterials Science, Bohdan Khmelnytsky National University, 18031, Cherkasy, Ukraine*

[e] *Tomsk State University, Lenin Avenue 36, Tomsk 634050, Russia*

[f] *College of Chemistry and Chemical Engineering, Henan University, Kaifeng, Henan 475004, P.R. China*

ABSTRACT: Magnetizabilities and magnetically induced current densities have been calculated and analyzed for a series of antiaromatic cyclo[4k]carbons (k=2-11), iso[n]phlorins

(n=4-8), expanded porphyrinoids and *meso–meso*, *β–β*, *β–β* triple linked porphyrin and isophlorin arrays. The cyclo[4k]carbons with k=2-6 are predicted to be closed-shell paramagnetic molecules due to the very strong paratropic ring current combined with its large radius. Larger cyclo[4k]carbons with k=6-11 are diamagnetic, because they sustain a paratropic ring current whose strength is weaker than -20 nA T^{-1}, which seems to be the lower threshold value for closed-shell paramagnetism. This holds not only for cyclo[4k]carbons, but also for other organic molecules like expanded porphyrinoids and oligomers of porphyrinoids. The present study shows that *meso–meso*, *β–β*, *β–β* triple linked linear porphyrin and isophlorin arrays have a domain-like distribution of alternating diatropic and paratropic ring currents. The strength of their local paratropic ring currents is weaker than -20 nA T^{-1} in each domain. Therefore, linear porphyrin and isophlorin arrays become more diamagnetic with increasing length of the ribbon. For the same reason, square-shaped *meso–meso*, *β–β*, *β–β* triple linked free-base porphyrin and isophlorin tetramers as well as Zn(II) complex of the porphyrin tetramer are diamagnetic. We show that closed-shell molecules with large positive magnetizabilities can be designed by following the principle that a strong paratropic current ring combined with a large ring-current radius leads to closed-shell paramagnetism.

1. INTRODUCTION

The aromaticity concept is manifested by molecular structure,[1] chemical reactivity,[2] spectroscopic properties,[3] magnetic properties,[4] and molecular conductivity.[5] A large number of

studies have shown that the degree of aromatic-city can be determined from magnetic shieldings,[6] ring-current strengths[7] and other molecular magnetic properties.[8-11] Electron delocalization and pathways of magnetically induced current densities provide information about molecular behaviour in the presence of an external magnetic field (**B**), which is important when designing novel magnetic materials.[12] The magnetic susceptibility (χ) also called magnetizability is a measure of interactions between matter and an external magnetic field (**B**).[13] The magnetizability (χ) is a second-rank tensor that can be formally divided into diamagnetic (χ^d) and paramagnetic (χ^p) contributions.[13-17] The magnetically induced current density (**J**), which is the first-order electronic response to an external magnetic field (**B**), can analogously be decomposed into diamagnetic ($\mathbf{J_{dia}}$) and paramagnetic ($\mathbf{J_{para}}$) current-density contributions.[16]

Since most closed-shell organic compounds are non-aromatic or aromatic, χ^p is in absolute value often smaller than χ^d. The magnetizability of organic molecules is then diamagnetic corresponding to negative magnetizability values, by definition. The more negative magnetizability, the stronger diamagnetic is the molecule. When χ^p dominates, the molecule is paramagnetic with a positive magnetizability. Paramagnetic molecules are in general open-shell molecules, whereas closed-shell paramagnetism (CSP) is rare.[13,18] Diatomic BH and its isoelectronic analogues CH^+ and BeH^- are known to be closed-shell paramagnetic molecules,[19-21] whereas only a few examples of closed-shell paramagnetic polyatomic molecules have been reported.[22,23]

We have shown in a number of recent studies that antiaromatic molecules sustaining a strong paratropic ring current can be closed-shell paramagnetic molecules,[24-26] which are spectroscopically characterized by intense low-lying magnetic-dipole-allowed electronic transitions. Strong paratropic ring currents also affect the magnetizability, because the angular momentum of the paratropic ring current increases the χ^p contribution. Anderson *et. al.*[23] recently detected CSP for closed-shell multicharged antiaromatic porphyrin nanorings, which experimentally confirmed that CSP can occur in strongly antiaromatic molecular rings.

The article is outlined as follows. In the next section, we briefly discuss the theory of closed-shell paramagnetism. In section 3, the employed computational methods are presented. These methods are applied in section 4.1 to a closed-shell paramagnetic tetra-cationic hexaporphyrin nanowheel, whose magnetizability has been measured experimentally. In section 4.2, we study the magnetizability and ring-current strengths of a series of antiaromatic cyclo[4k]carbon rings. In section 4.3 we discuss magnetic properties of porphyrinoid arrays, while the data for expanded isophlorins and expanded porphyrinoids are presented in sections 4.4 and 4.5, respectively. The aromaticity of the square-shaped [36]octaphyrin(1.1.1.1.1.1.1.1) and cyclo-octafuran(1.1.1.1.1.1.1.1) is discussed in section 4.6. The obtained results are summarized and concluded in section 5.

2. THEORY

Molecular magnetizability is generally calculated as the second derivative of the electronic energy with respect to the strength of the external magnetic field using the response formalism.[27-29] However, the mechanism of closed-shell paramagnetism can be easier understood from the sum over states expression for the second derivative, where the magnetizability is split into diamagnetic (χ^d) and paramagnetic (χ^p) contributions[30]

$$\chi_{\alpha\beta} = -\frac{1}{4}\sum_i \langle 0|\, r_{Oi}^2\delta_{\alpha\beta} - r_{Oi\alpha}r_{Oi\beta})|0\rangle + \frac{1}{2}\sum_{\substack{i \\ K>0}} \frac{\langle 0|\,(\boldsymbol{r}_{Oi}\times\boldsymbol{p}_i)_\alpha|K\rangle\langle K|\,(\boldsymbol{r}_{Oi}\times\boldsymbol{p}_i)_\beta|0\rangle}{E_K - E_0} \quad (1)$$

The summation in Eq (1) runs over all electrons i and excited states K. $\boldsymbol{r}_{Oi} = \boldsymbol{r}_i - \boldsymbol{r}_O$ is the distance from the common gauge origin, $\boldsymbol{p}_i$ is the momentum operator, and E_0 and E_K are the energy of the ground and exited states, respectively. The diamagnetic term is always negative and depends only on the ground state, whereas the paramagnetic part contains the orbital angular momentum operator and is always positive. Low-lying excited states with large magnetic transition moments from the ground state have large paramagnetic contributions to the magnetizability. These excited states have also been found to be the reason for the antiaromatic character of isophlorin and other antiaromatic porphyrinoids.[26]

Magnetizabilities can also be obtained by integrating the magnetically induced current density multiplied with the vector potential of the external magnetic field:[16, 31]

$$\chi_{\alpha\delta} = -\frac{1}{2c}\varepsilon_{\alpha\beta\gamma}\int r_\beta J_\gamma^{B\delta}(\boldsymbol{r})\,\mathrm{d}\mathbf{r}, \quad (2)$$

where $\varepsilon_{\alpha\beta\gamma}$ is the Levi-Civita tensor, r_β is the vector potential and $J_\gamma^{B\delta}(\boldsymbol{r})$ is the magnetically induced current density susceptibility that we call current density in the rest of this article. When the external magnetic field is applied in *z* direction, χ_{zz} is obtained as:

$$\chi_{zz} = -\frac{1}{2c}\int (x\, J_y^{B_z}(\boldsymbol{r}) - y J_x^{B_z}(\boldsymbol{r}))\, d\boldsymbol{r} \quad (3)$$

When a planar aromatic molecule lies in the *xy* plane, $J_y^{B_z}(\boldsymbol{r})$ flows in the positive *y* direction for positive *x* values and in the negative *y* direction when x is negative, leading to a negative contribution to χ_{zz}. The second term in Eq. (3) is also negative for aromatic molecules. The paratropic ring current of antiaromatic molecules flows in the opposite direction and results in positive contributions to χ_{zz}. The two contributions in Eq. (3) are large for strong ring currents whose radius is large. For ring-shaped molecules the χ_{xx} and χ_{yy} elements of the magnetizability tensor are negative as for most molecules and they scale nearly linearly with the size of the molecule as originally observed by Pascal.[32] The average molecular magnetizability is calculated as the trace of the magnetizability tensor:

$$\chi = \frac{1}{3}(\chi_{xx} + \chi_{yy} + \chi_{zz}) \quad (4)$$

implying that the paramagnetic χ_{zz} contribution of antiaromatic molecules in the *xy* plane is cancelled by the diamagnetic contributions from $\chi_{xx} + \chi_{yy}$. The magnetizability is positive when χ_{zz} is larger than the absolute value of $\chi_{yy} + \chi_{xx}$. We have previously shown that porphyrinoids become closed-shell paramagnetic when the strength of the paratropic ring current exceeds -20 nA T^{-1},[24] which holds for molecules with about the same radius of the ring current as isophlorin.

3. COMPUTATIONAL METHODS

The molecular structures were optimized at the density functional theory (DFT) level using the M06-2X exchange–correlation functional[33] and the def2-TZVP basis set[34]. It is known that this hybrid functional well describe magnetic properties and magnetizabilities.[35-36] The NMR shielding constants were calculated by using the Gauge Including Atomic Orbital (GIAO) method[37] at the M06-2X level of theory. These calculations were performed for isolated molecules using the Gaussian 16 program package.[38]

The GIMIC program[39,40] was used for calculation of the magnetically induced current densities and the integrated current densities. The magnetically induced current densities were calculated using density matrices obtained in the NMR shielding calculations and basis-set data. The magnetic field was oriented perpendicular to the molecular plane. The strengths of the current densities were obtained by numerical integration of the current density passing a rectangular surface perpendicular to the molecule plane. The magnetizability was also calculated using GIMIC.

We performed state-specific complete active space self-consistent field (SS-CASSCF) calculations for free-base porphyrin arrays $(\mathbf{H_2P})_n$ and isophlorin arrays $(\mathbf{IPh})_n$ with n=1,2,3,4. The SS-CASSCF calculations included 8 electrons in 8 molecular orbitals (MO). The weight of closed shell determinant varies in the range of 0.9-0.93. For other determinants, they are less than 0.15 implying that the studied molecules are single-reference systems. The SS-CASSCF calculations were carried out with the def2-TZVP basis set using the Firefly software.[41]

4. RESULTS AND DISCUSSION

4.1 Hexaporphyrin nanowheel. The experimentally measured magnetizability of the recently synthesized tetra-cationic hexaporphyrin nanowheel (**c-P6·T6**$^{4+}$) in Figure 1 is 4418 a.u.[23] Our calculations at the M06-2X/def2-TZVP level yield a magnetizability of 3188 a.u. suggesting that DFT calculations using the M06-2X functional slightly underestimate the magnetizability of the strongly antiaromatic molecules. Previous calculations on antiaromatic expanded porphyrins showed that density functionals with less than 50% Hartree-Fock exchange tend to overestimate the strength of the paratropic ring current of strongly antiaromatic molecules.[42] A large positive magnetizability is obtained for **c-P6·T6**$^{4+}$, because it sustains a strong paratropic ring current of -65 nA T^{-1} whose radius is 13 Å. A larger positive magnetizability can be obtained by either increasing the radius of the ring current or by increasing the strength of the paratropic ring current. However, the diamagnetic contribution to the magnetizability also increases with increasing size of the molecule according to Pascal's rule. Closed-shell paramagnetism relies on the balance between the paramagnetic contribution from χ_{zz} and the diamagnetic contributions from the χ_{xx} and χ_{yy} terms.

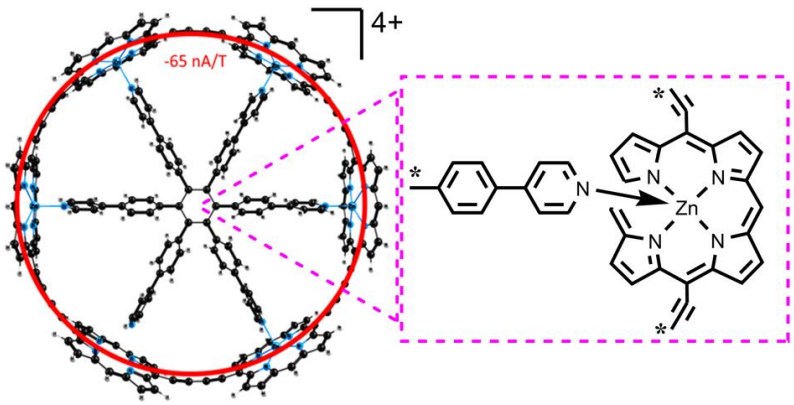

Figure 1. The molecular structure of the tetra-cationic hexaporphyrin nanowheel (**c-P6·T6**$^{4+}$).[23] The paratropic ring current circulation pathway is schematically indicated with the red ring with an average radius 13 Å.

4.2 Cyclo[n]carbons. The magnetizability and ring-current strengths have been also studied for a series of all-carbon molecules consisting of antiaromatic cyclo[n]carbons, *i.e.,* cyclic C_n polyynes (n=4*k*, with *k*=2-11) that satisfy Hückel's rule for antiaromaticity. The obtained results are summarized in Table 1. The calculations show that the strength of the induced paratropic ring current decreases with increasing number of carbon atoms and becomes diatropic for the two largest all-carbon rings. Since the radius of the molecular ring increases with the number of carbons, the product of the radius times the ring current strength passes through a maximum for n=20 (*k*=5), which also has the largest χ_{zz} value of 105 a.u. The magnetizability is positive for *k*=2-6, whereas the larger polyynes are diamagnetic, because χ_{xx} and χ_{yy} are negative and they increase in absolute value linearly with the size of the molecule. The calculations show that cyclo[4*k*]carbons with *k*=2-6 are closed-shell paramagnetic molecules. Cyclo[28]carbon is diamagnetic even though it has a radius of 5.7 Å and sustains a strong paratropic ring current of -15 nA T^{-1}, because the sum of the diamagnetic contributions from χ_{xx} and χ_{yy} of -84 a.u. is larger than the paramagnetic χ_{zz} contribution of 67 a.u. Cyclo[44]carbon molecule, which is the largest all-carbon ring that we studied, is slightly aromatic with a ring-current strength of 4 nA T^{-1} resulting in diamagnetism with a magnetizability of -59 a.u.

Annulenes with (4k+2) π electrons exhibit a more stable π system with Hückel topology and those with (4k) π electrons prefer a Möbius twisted structure.[43] Cyclo[n]carbons (n=4k) become aromatic for large n values due to the change from Hückel to Möbius topology of the conjugated π electrons. Constructing Frost-Musulin mnemonic diagrams shows that cyclo[4n]carbons can be actually considered as double [n]annulenes, whose π electrons are oriented orthogonally to the molecular plane and in the plane, respectively.[44-46] With increasing ring size (n), the difference between the Frost-Musulin mnemonic of the Hückel system (the vertex of the n-gon is its lowest point) and the one for the Möbius system (the lowest edge is horizontal) becomes smaller leading to almost the same π-electron energy. For n=36 (k=9) and n=40 (k=10), the cyclo[n]carbons are non-aromatic sustaining very weak ring currents of -0.5 and 0.9 nA T^{-1}, respectively, implying that the antiaromatic Hückel (4k) and the aromatic Möbius (4k) structures are degenerate. For n=44 (k=11), Möbius aromaticity clearly dominates over the Hückel antiaromaticity leading to a diatropic ring current of 4.0 nA T^{-1}.

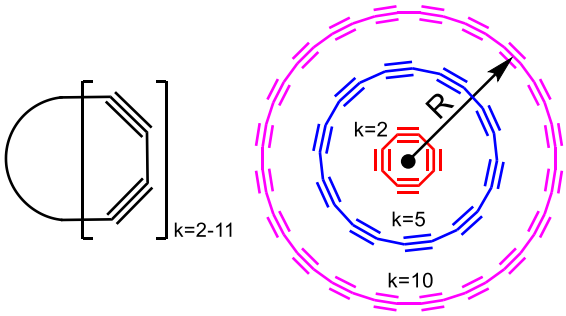

Figure 2. The formal molecular structures of the studied cyclo[n]carbons (n=4*k*). The smallest studied molecule is cyclo[8]carbon (*k*=2) and the largest one is cyclo[44]carbon (*k*=11).

Table 1. The ring-current strength (J in nA T^{-1}), the radius of the ring current (R in Å), and the average magnetizability (χ in a.u.) of the studied cyclo[n]carbons.

n	J	R	χ
8	-42	1.8	5
12	-40	2.4	14
16	-36	3.5	18
20	-27	4.1	16
24	-18	4.9	7
28	-15	5.7	-6
32	-4.4	6.5	-20
36	-0.5	7.4	-34
40	0.9	8.4	-47
44	4.0	9.1	-59

4.3 Porphyrinoid arrays. Free-base porphyrin $(\mathbf{H_2P})_0$ is an aromatic and diamagnetic molecule with χ = -68 a.u.[24,25,47-49] It sustains a global diatropic magnetically induced ring current of 27 nA T^{-1} by the 26 delocalized π electrons.[28] Isophlorin $(\mathbf{IPh})_0$ is chemically stable and strongly antiaromatic sustaining a ring current of -27 nA T^{-1} by its 28 π electrons.[24] Isophlorin is weakly paramagnetic with a positive magnetizability of 12 a.u. at the M06-2X level of theory and of 16 a.u. at the MP2 level.[24] We have investigated how the magnetizability changes when extending porphyrin and isophlorin into the one-dimensional (1D) *meso–meso*, *β–β*, *β–β*-linked arrays shown in Figure 3. In 2001, Osuka *et al*., synthesized and fully characterized a *meso–meso*, *β–β*, *β–β*-linked porphyrin consisting of twelve Zn-porphyrin (**ZnP**) moieties (n=11)[50]. Eight years later same group synthesized fully conjugated porphyrin tapes consisting of 24 **ZnP** moieties.[51]

We have studied the current density of different moieties of the 1D $(\mathbf{IPh})_n$ arrays, because total ring-current strengths are less meaningful. We found that the **IPh** arrays have a very

unusual mixed aromatic-antiaromatic character. Analysis of the current-density pathways in the **IPh** arrays indicates the presence of a strong almost independent paratropic ring current of -24 nA T^{-1} inside each **IPh** moiety. A weak diatropic ring current is sustained by the naphthalene ring between the two **IPh** moieties. Longer $(\mathbf{IPh})_n$ arrays (n=2-7) also sustain localized paratropic ring currents in each **IPh** moiety. However, the paratropic ring currents in the inner **IPh** fragments are somewhat weaker than the ones at the end of the **IPh** moieties. The mixed aromatic-antiaromatic character suppresses the global electron delocalization in the $(\mathbf{IPh})_n$ arrays, which is supported by the almost size-independent HOMO-LUMO gap (HLG) of the $(\mathbf{IPh})_n$ arrays (Table 2). Thus, there is no quantum confinement effect for longer $(\mathbf{IPh})_n$ arrays, which is unexpected but can be explained in terms of alternating local diatropic and paratropic ring currents. The calculations also show that the $(\mathbf{IPh})_n$ arrays have several quasi-degenerated low-lying excited states that are accessible through magnetic-dipole transitions.

Calculations on the $(\mathbf{H_2P})_n$ arrays show that local paratropic ring currents are confined in the molecular moieties between the porphyrin subunits (Figure 4), whereas the porphyrin rings sustain weak diatropic ring currents. The global delocalization of the π electrons leads to a small non-vanishing diatropic ring current of 6 nA T^{-1} that flows along the central β-β C-C link, which results in a smaller HLG for the longer $(\mathbf{H_2P})_n$ arrays. The small HLG leads to a stronger paratropic ring currents than for the $(\mathbf{IPh})_n$ arrays that do not sustain any ring-current flux along the central β-β C-C link, which is denoted with the dashed line in Figure 4. The weak global ring current of 6 nA T^{-1} for the $(\mathbf{H_2P})_n$ arrays suggests that they have a

global electron delocalization leading to a decreasing HLG for longer arrays in contrast to the $(\mathbf{IPh})_n$ arrays, which do not sustain any global ring current. Thus, the $(\mathbf{IPh})_n$ arrays lack global electron delocalization, which results in a size-independent HLG.

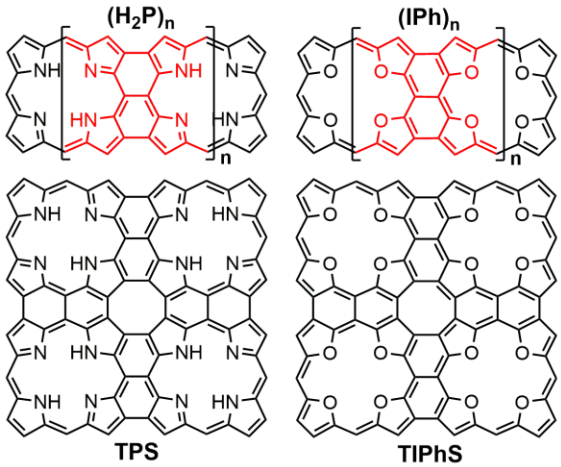

Figure 3. The molecular structures of the studied porphyrin (**H_2P**) and isophlorin (**IPh**) arrays. Top chart represents linear oligomers $(\mathbf{H_2P})_n$ and $(\mathbf{IPh})_n$ (n=0-7), while in the bottom part shows the square-shaped **TPS** and **TIPhS** arrays.

The $(\mathbf{H_2P})_n$ arrays are diamagnetic because the strengths of the local paratropic ring currents in the naphthalene-pyrrole moieties are less than 20 nA T^{-1}, which has been found to be the critical ring-current strength for closed-shell paramagnetism of porphyrinoids. The diatropic ring currents in the porphyrin rings also cancel the paramagnetic contribution to χ_{zz}. The $(\mathbf{IPh})_n$ species exhibit a diamagnetic character due to same reason namely, the strength of the local paratropic ring currents in the isophlorin fragments is less than threshold value of -20 nA T^{-1} and diatropic ring currents in the naphthalene moieties between the isophlorin rings cancel the paramagnetic contribution to χ_{zz}. However, the magnetizability of $(\mathbf{IPh})_n$

is less diamagnetic than for the $(\mathbf{H_2P})_n$ analogues (-11 *vs.* -96 a.u. for n=1, -127 *vs.* -30 a.u. for n=2, etc., see Table 2). Thus, if one would be able to slightly increase the strength of the local paratropic ring current in each isophlorin unit, the whole array might become paramagnetic.

Table 2. The magnetizability (χ in a.u.) and the HOMO-LUMO gap (HLG in eV) of the studied porphyrin $(\mathbf{H_2P})_n$ and isophlorin $(\mathbf{IPh})_n$ arrays. HLG represents the smallest denominator in the expression for χ_p. The ring-current strengths of porphyrin and isophlorin are 27 nA T^{-1} and -29 nA T^{-1}, respectively.

	$(\mathbf{H_2P})_n$		$(\mathbf{IPh})_n$	
n	χ	HLG	χ	HLG
0	-68	4.46	12	3.39
1	-96	2.82	-11	2.22
2	-127	2.16	-30	2.17
3	-158	1.77	-48	2.14
4	-190	1.50	-68	2.14
5	-221	1.28	-87	2.12
6	-252	1.06	-106	2.12
7	-283	0.61	-124	2.11

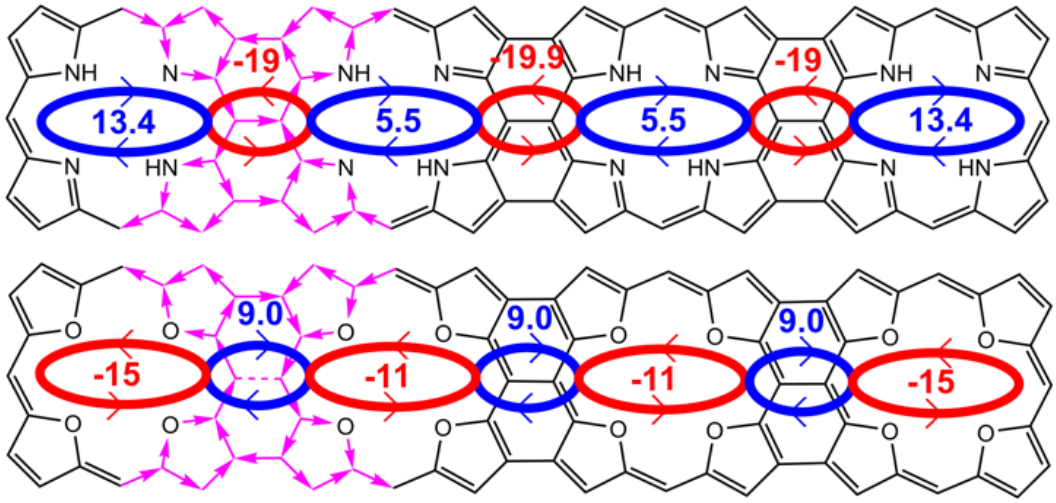

Figure 4. The strong local paratropic ring currents (red ellipses) and the weak diatropic ring currents (blue ellipses) in the $(\mathbf{H_2P})_3$ and $(\mathbf{IPh})_3$ arrays (top and bottom, respectively). The structure of the current-density flow is the same for the whole series of the studied molecules (n=1-7). The pink arrows show the current-density pathways, and numbers correspond to strength of the ring currents (in nA T^{-1}).

We also studied the current density and magnetizability of two-dimensional (2D) quadratic $\mathbf{H_2P}$ (**TPS**) and **IPh** (**TIPhS**) sheets (Figure 5) in which the building blocks are connected by the same *meso–meso*, *β–β*, *β–β*-linking scheme as in the linear arrays. Free-base **TPS** has been successfully synthesized and characterized by Osuka *et.al.,*[52,53] while **TIPhS** is predicted here. **TPS** and **TIPhS** are predicted to sustain ring currents along the outer edge (rim) of the molecule and in the inner eight-membered ring (hub). In contrast to the $(\mathbf{H_2P})_n$ and $(\mathbf{IPh})_n$ arrays, no multiple paratropic ring-current domains were found in the quadratic 2D sheets. The calculations show that the ring current of the hub of **TPS** and **TIPhS** is paratropic (Figure 5), which agrees with previous NICS studies on **TPS**[53] and with studies showing that hetero[8]circulenes also generally sustain a strong paratropic ring current in the hub.[54-56] Complexation of free-base **TPS** with Zn^{2+} yields tetra-Zn-porhyrin Zn_4**TPS**[57,58], where the eight inner hydrogens are replaced by four Zn^{2+} cations. The complexation enhances the paratropic ring currents in the hub increasing the ring-current strength from -33 nA T^{-1} for free-base **TPS** to -65 nA T^{-1} for Zn_4**TPS**. The diatropic ring current of 5 nA $T^{-1}$and 7 nA T^{-1} along the rim of **TPS** and Zn_4**TPS**, respectively, are much weaker than the paratropic ones in the hub (Figure 5). However, due to the large radius of

the diatropic ring current of the rim, they play a crucial role for the sign of the magnetizability of **TPS** and Zn_4**TPS**. The paramagnetic contribution from the strong paratropic ring current of the hub with a small radius is cancelled by the diamagnetic contribution from the weak diatropic ring current with a large radius. In addition, each atom brings diamagnetic contributions to the magnetizability according to Pascal's rule. Therefore, free-base **TPS** and the corresponding Zn_4**TPS** complex are diamagnetic with magnetizabilities of -126 a.u. and -132 a.u., respectively. Due to the same reason, **TIPhS** sustains a paratropic ring current of -11 nA T^{-1} in the hub and a diatropic ring current of 12 nA T^{-1} along the rim leading to a diamagnetic molecule with a negative magnetizability of -140 a.u.

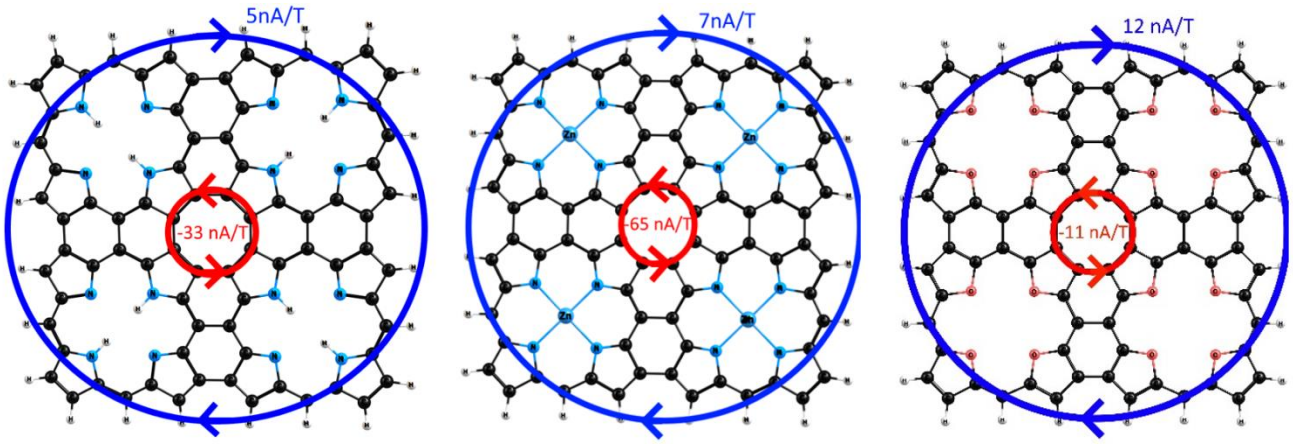

Figure 5. The diatropic (blue line) and paratropic (red line) magnetically induced ring currents in the free-base tetra-porphyrin **TPS** sheet (left), the Zn_4**TPS** sheet (middle), and in the tetra-isophlorin **TIPhS** sheet (right).

4.4 Iso[n]phlorins. The magnetizability and ring-current strengths were calculated for isophlorin **IPh** (iso[4]phlorin) and a series of analogous expanded isophlorins (Figure 6). The molecular charge has been chosen such that the expanded isophlorins fulfill Hückel's rule

for antiaromaticity. Isophlorin is an antiaromatic porphyrin with 28 π electrons in the porphyrin ring. Originally isophlorin was constructed from free-base porphyrin by adding two inner hydrogens.[59] Alternatively, one can replace the NH moieties with iso-electronic oxygen atoms.[60-62] The expanded isophlorins studied here consisting of 5-8 furan rings have not been synthesized, whereas the synthesized cyclo-octafuran(1.1.1.1.1.1.1.1) has inverted furan rings.[63] Our calculations show that the inverted (experimental) configuration is 210 kcal mol^{-1} more favourable than a hypothetical circle-shaped iso[8]phlorin. For the design of closed-shell paramagnetic antiaromatic molecules, we have considered a series of iso[n]phlorins of the same circle-shaped topology. Calculations on this series of molecules yield a relation between the ring-current strength, the ring-current radius and the magnetizability. We have previously showed that the isophlorin ring consisting of four furan rings connected via methine groups is strongly antiaromatic sustaining a paratropic ring current of -63 nA T^{-1} at the B3LYP level.[48] The present M06-2X calculations yield a ring-current strength of -29 nA T^{-1} for isophlorin. The magnetizability of isophlorin calculated at the M06-2X level is 12 a.u. The calculated ring-current strengths and magnetizabilities of the antiaromatic (n=4*k*) expanded isophlorins are summarized in Table 3. The studied isophlorins sustain strong paratropic ring currents that are of about the same strength except for iso[8]phlorin, which sustains a very strong paratropic ring current of -617 nA T^{-1}. Since the radius increases with the number of furan rings, the magnetizability also increases with n. For iso[8]phlorin the large radius of the ring current of 5.3 Å and the strong paratropic ring current lead to a very large positive magnetizability of 3532 a.u.

Table 3. The ring-current strength (J in nA T^{-1}), the radius of the ring current (R in Å), and the average magnetizability (χ in a.u.) of the studied iso[n]phlorins, where n is the number of furan rings.

Molecule	J	R	χ
Iso[4]phlorin	-29	2.0	12
Iso[5]phlorin^{1+}	-73	2.5	132
Iso[6]phlorin^{2+}	-56	3.7	140
Iso[7]phlorin^{1-}	-45	4.5	158
Iso[8]phlorin	-617	5.3	3532[a]

[a] For comparison, the magnetizability of **c-P6·T6**$^{4+}$ is 4418 a.u.[22] and the magnetizability of O_2 ($^3\Sigma_g$) is 719 a.u. at a temperature of 293 K.[64]

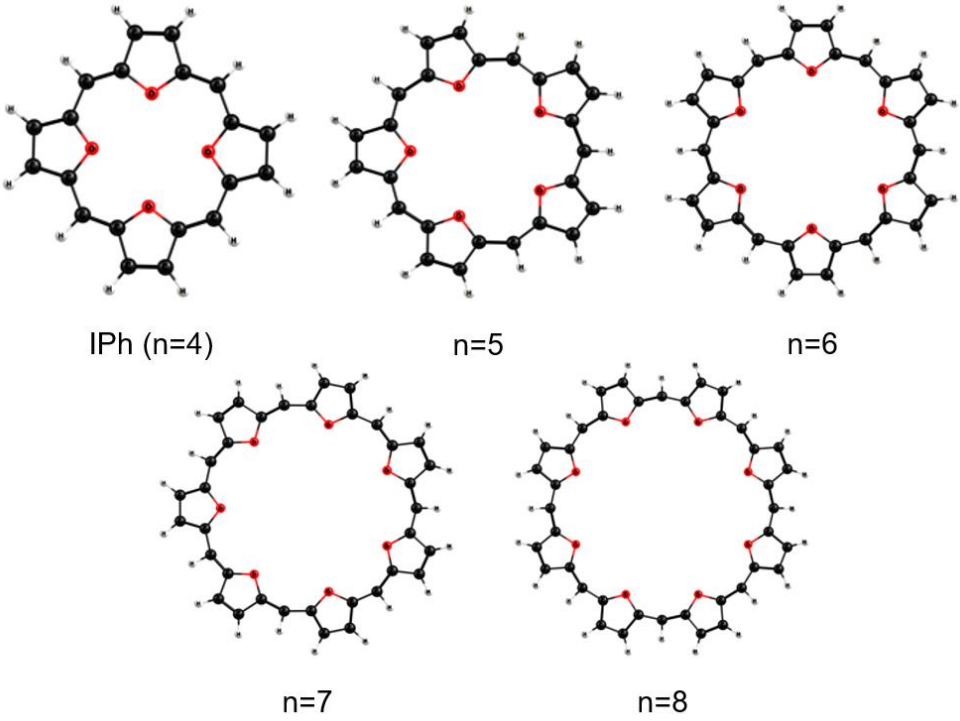

Figure 6. The molecular structures of the studied iso[n]phlorins, n=4-8.

4.5. Expanded porphyrinoids. We also studied orangarin, rosarin, and amethyrin, which are synthesized expanded antiaromatic porphyrins whose molecular structures are shown in Figure 7.[65] Even though they are strongly antiaromatic,[41] calculations of the magnetizabilities show that they are diamagnetic (Table 4). The paratropic ring currents are weaker

than -20 nA T^{-1} and the radius of the ring current is not large enough to lead to closed-shell paramagnetism.

We also studied the hypothetic circle-shaped [40]octaphyrin(1.1.1.1.1.1.1.1) molecule with eight NH groups that consists of eight pyrrole rings connected *via* methine bridges. The molecular structure of [40]octaphyrin(1.1.1.1.1.1.1.1) shown in Figure 7d is a local minimum on the potential energy surface of the singlet ground state; it lies 163 kcal mol^{-1} above the square-shaped [40]octaphyrin(1.1.1.1.1.1.1.1) shown in Figure 8b also containing eight NH groups, which has not been synthetized. [40]octaphyrin(1.1.1.1.1.1.1.1) with inverted pyrrole rings is diamagnetic with a negative magnetzability of -67 a.u. and practically nonaromatic sustaining a ring current of J=3.4 nA T^{-1}. In contrast, the circle-shaped [40]octaphyrin(1.1.1.1.1.1.1.1) sustains a strong paratropic ring current of -561 nA T^{-1} resulting in a large positive magnetizability of 3244 a.u.

Table 4. The ring-current strength (J in nA T^{-1}), the radius of the ring current (R in Å), and the average magnetizability (χ in a.u.) of orangarin, rosarin, amethyrin and the hypothetic [40]octaphyrin(1.1.1.1.1.1.1.1).

Molecule	J	R	χ
Orangarin	-20	2.0	-7.0
Rosarin	-18	2.5	-4.9
Amethyrin	-14	2.5	-14
[40]octaphyrin(1.1.1.1.1.1.1.1) (circle-shaped)	-561	5.3	3244

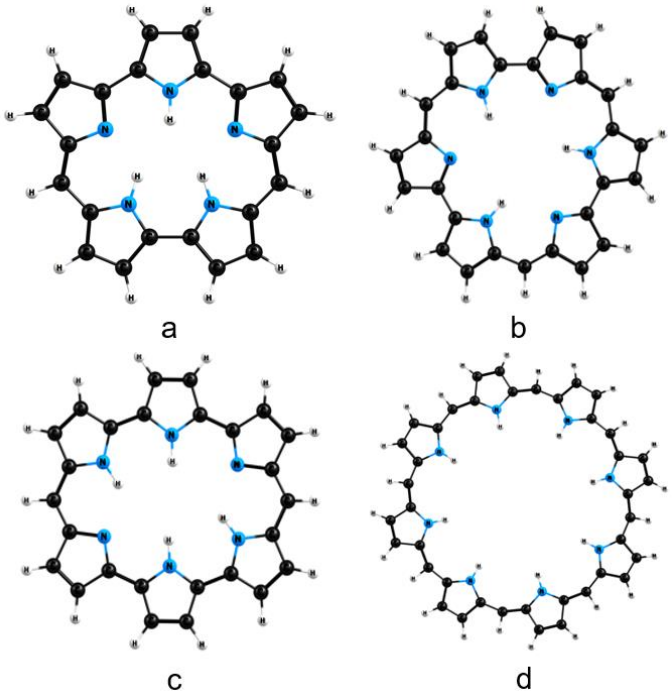

Figure 7. The molecular structure of the antiaromatic expanded porphyrins: a) orangarin b) rosarin c) amethyrin and d) circle-shaped [40]octaphyrin(1.1.1.1.1.1.1.1).

The anomalously high paratropic ring currents for the hypothetical iso[8]phlorin in Figure 6 and [40]octaphyrin(1.1.1.1.1.1.1.1) in Figure 7d seem to originate from the circular topology of the molecular structure. They are examples of closed-shell paramagnetic molecules with a strong ring current and a large ring-current radius. Since iso[8]phlorin and circle-shaped [40]octaphyrin(1.1.1.1.1.1.1.1) are strongly antiaromatic, they are high-lying local minima on the potential energy surfaces of the singlet ground state. The global minimum structure has four pyrrole/furan rings with the NH/O moiety pointing inwards and four NH/O moieties pointing outwards. The synthesis of the high-lying structures is certainly challenging, whereas from the electronic structure point of view these molecules are stable.

4.6. Square-shaped [36]octaphyrin(1.1.1.1.1.1.1.1) and cyclo-octafuran(1.1.1.1.1.1.1.1)

The previously synthesized [36]octaphyrin(1.1.1.1.1.1.1.1)[66] and cyclo-octafuran(1.1.1.1.1.1.1.1)[63] with inverted rings shown in Figure 8 are weakly aromatic and weakly antiaromatic molecules sustaining a weak diatropic (2.4 nA T^{-1}) and weak paratropic (-3.8 nA T^{-1}) global ring current, respectively. Cyclo-octafuran (1.1.1.1.1.1.1.1)[63] is a planar diamagnetic molecule with a magnetizability of -56 a.u. It sustains local diatropic ring currents of 5.9 and 8.8 nA T^{-1} in the furan rings. The [36]octaphyrin(1.1.1.1.1.1.1.1)[66] molecule shown in Figure 8c (it contains four NH groups in contrast to hypothetical [36]octaphyrin(1.1.1.1.1.1.1.1) in Figure 8b) is also planar and diamagnetic molecule with a magnetizability of -9.7 a.u. It is a weakly antiaromatic 40 π electron annulene, since the N/NH moieties do not contribute to the global ring current due to the local ring currents in the pyrrole rings. When two protons are removed from [36]octaphyrin(1.1.1.1.1.1.1.1) (Figure 8d), the resulting dianion is antiaromatic with a ring-current strength of -7 nAT^{-1} and paramagnetic with a magnetizability of χ=9 a.u. It is a porphyrinoid with 46 π electrons showing that large molecular rings sustaining relatively weak paratropic ring currents can be closed-shell paramagnetic molecules. The optimized molecular structure of the [36]octaphyrin(1.1.1.1.1.1.1.1) dianion is ruffled, while in the single-crystal X-ray diffraction measurement, the dianion with C_6F_5 substituents in the *meso*-positions and with tetrabutylammonium counterions is nearly planar. Thus, we propose that the unsubstituted [36]octaphyrin(1.1.1.1.1.1.1.1) dianion is a Möbius-antiaromatic 46 π electron molecule.

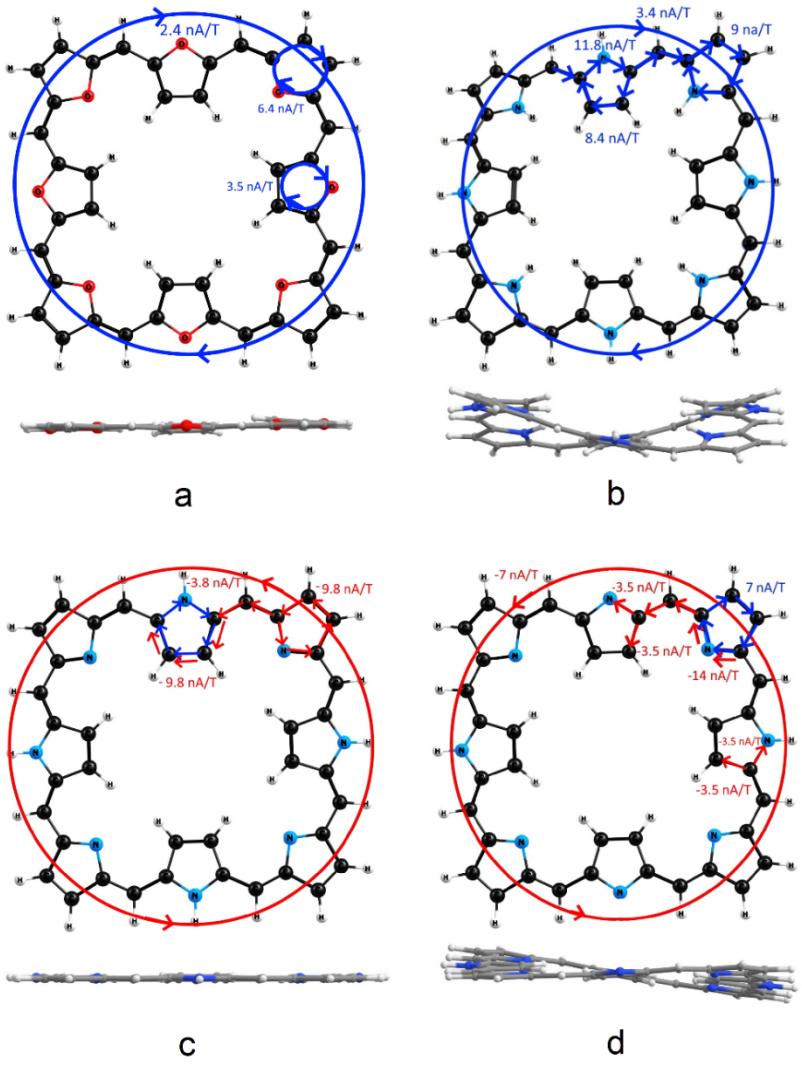

Figure 8. Current-density pathways and ring-current strengths calculated for (a) cyclo-octafuran(1.1.1.1.1.1.1.1), (b) hypothetical square-shaped [40]octaphyrin(1.1.1.1.1.1.1.1), (c) [36]octaphyrin(1.1.1.1.1.1.1.1) and (d) [36]octaphyrin(1.1.1.1.1.1.1.1) dianion using GIMIC. The side view of the molecular structures are also shown.

CONCLUSIONS

The present study gives a recipe for designing closed-shell paramagnetic molecular rings. One of the prerequisites for closed-shell paramagnetism (CSP) of ring-shaped porphyrinoids seems to be that they sustain a paratropic ring current of at least -20 nA T^{-1}. The paratropic

ring current must not be cancelled by other diatropic ring currents with larger radii. Larger radii of the paratropic ring current lead to stronger closed-shell paramagnetism. However, the diamagnetic contribution to the magnetizability also increases with the size of the ring according to Pascal's rule. For planar molecules in the *xy* plane, the *zz* component of the magnetizability tensor can be positive due to a strong paratropic magnetically induced ring current, whereas the *xx* and *yy* components are negative (diamagnetic) according to Pascal's rule, since planar molecules do not sustain any paratropic ring currents when the magnetic field is parallel to the molecular plane. Thus, closed-shell paramagnetism is a balance between the paramagnetic contribution to the *zz* element of the magnetizability tensor and the diamagnetic contributions from the *xx* and *yy* elements.

The reliability of the employed computational level was assessed by calculating the magnetizability of the recently synthesized tetra-cationic hexaporphyrin nanowheel (**c-P6·T6**$^{4+}$), which is a closed-shell paramagnetic molecule with an experimental magnetizability of 4418 a.u.[23] Calculations at the M06-2X yielded a magnetizability of 3188 a.u. showing that the employed computational level is able to reproduce the large positive magnetizability of **c-P6·T6**$^{4+}$. Magnetizabilities calculated at the M06-2X level for closed-shell paramagnetic molecular rings seem though to be slightly underestimated.

Iso[4]phlorin sustaining a ring current of -29 nA T^{-1} with a radius of 2 Å is paramagnetic with a magnetizability of 12 a.u. Cyclo[8]carbon with a radius of 1.8 Å sustaining a ring current of -42 nA T^{-1} is weakly paramagnetic with a magnetizability of 5 a.u. These examples show that closed-shell paramagnetic molecular rings with a radius of < 2Å must sustain a very strong paratropic ring current.

A series of *meso–meso*, *β–β*, *β–β*-linked porphyrins (**TPS**) and isophlorins (**IPh**) extending in one (arrays) and two (sheets) dimensions were studied. The linear and square-shaped porphyrin and isophlorin sheets have a different topology of the ring currents. The linear porphyrinoid arrays have multiple centers sustaining local diatropic and paratropic ring currents, whereas the squared-shaped porphyrinoid sheets sustain a paratropic ring current in the hub and a diatropic ring current along the rim. Substituting the inner NH protons of **TPS** with Zn^{2+} cations leads to a stronger paratropic ring current in the hub, whereas the diatropic ring current along the rim is less affected.

The linear isophlorin arrays $(\mathbf{IPh})_n$ sustain paratropic ring currents in each of the isophlorin moieties and a diatropic ring current in the naphthalene moieties between the isophlorins. The $(\mathbf{IPh})_n$ arrays do not sustain any global ring current. The absence of global electron delocalization leads to a very weak quantum confinement for the $(\mathbf{IPh})_n$ arrays implying that the HOMO-LUMO gap is almost independent of the number of isophlorins moieties for the longer $(\mathbf{IPh})_n$ arrays.

For the $(\mathbf{H_2P})_n$ arrays, a global diatropic ring current through the *β-β* links results in a smaller HOMO-LUMO gap for the longer $(\mathbf{H_2P})_n$ arrays. The porphyrin moieties sustain local diatropic ring currents, whereas the linking naphthalene-pyrrole moieties sustain local paratropic ring currents. The linear arrays sustaining several local paratropic ring currents are diamagnetic, because the ring-current strengths do not exceed -20 nA T^{-1}. Several paratropic ring currents in the same molecule does not make them paramagnetic, because the diamagnetic contribution increases also linearly with the number of atoms in the molecule.

Calculations on a series of expanded isophlorins fulfilling Hückel's rule for antiaromaticity show that they are paramagnetic due to the strong paratropic ring current and the large radius of the ring current. The largest member of the series namely iso[8]phlorin has a magnetizability of 3532 a.u., because it sustains a very strong ring current of -617 nA T^{-1} whose radius is 5.3 Å. Calculations on expanded porphyrins fulfilling Hückel's rule for antiaromaticity show that orangarin, rosarin, amethyrin are diamagnetic, since they sustain paratropic ring currents that a weaker than -20 nA T^{-1}. The largest member of that series is the hypothetic circle-shaped [40]octaphyrin(1.1.1.1.1.1.1.1) that sustains a strong paratropic ring current of -561 nA T^{-1} whose radius is 5.3 Å. The circle-shaped [40]octaphyrin(1.1.1.1.1.1.1.1) molecule is therefore strongly paramagnetic with a magnetizability of 3244 a.u.

AUTHOR INFORMATION

Corresponding Author

E-mail: glibar@kth.se, rashid.valiev@helsinki.fi

Notes

The authors declare no competing financial interests.

ACKNOWLEDGMENT

This work has been supported by the Olle Engkvist Byggmästare foundation (contract no. 189-0223) and by the Ministry of Education and Science of Ukraine (project no. 0117U003908). The calculations were performed with computational resources provided by the High-Performance Computing Center North (HPC2N) in Umeå, Sweden, through

the project "Multiphysics Modeling of Molecular Materials" SNIC 2019-2-41. The GIMIC calculations were carried out using the SKIF supercomputer at the Tomsk State University. This project has also been funded by the Academy of Finland through projects 1315600 and 314821. R.R.V. thanks the Tomsk Polytechnic University Competitiveness Enhancement Program (VIU-RSCABS-142/2019) for support. R.T.N. thanks Russian Scientific Foundation (18-19-00268)

ASSOCIATED CONTENT

Supporting Information

The Supporting Information is available free of charge on the ACS Publications website at DOI: 10.1021/acs.jpcc.XXXXXXX. Optimized geometries (Cartesian coordinates) for all studied molecules (c-P6·T6^{4+} nanowheel, cyclo[n]carbons (n=8, 12, 16 ... 44), $(H_2P)_n$ (n=0-7) and $(IPh)_n$ (n=0-7) arrays, TPS, Zn_4TPS and TIPhS nanosheets, iso[n]phlorins (n=4-8), expanded porphyrinoids, octaphyrins and cyclo-octa furans).

REFERENCES

(1) Krygowski, T. M., Cyrański, M. K. Structural Aspects of Aromaticity, *Chem. Rev.* **2001**, *101*, 1385–1420.

(2) Mucsi, Z.; Viskolcz, B.; Csizmadia, I. G. A Quantitative Scale for the Degree of Aromaticity and Antiaromaticity: A Comparison of Theoretical and Experimental Enthalpies of Hydrogenation, *J. Phys. Chem. A*, **2007**, *111* 1123–1132.

(3) Shin, J.-Y.; Kim, K. S.; Yoon, M.-C.; Lim, J. M.; Yoon, Z. S.; Osuka, A.; Kim D. Aromaticity and Photophysical Properties of Various Topology-Controlled Expanded Porphyrins, *Chem. Soc. Rev.* **2010**, *39*, 2751–2767.

(4) Gershoni-Poranne, R.; Stanger, A. Magnetic Criteria of Aromaticity, *Chem. Soc. Rev.* **2015**, *44*, 6597–6615.

(5) Fujii, S.; Marqués-González, S.; Shin, J.-Y.; Shinokubo, H.; Masuda, T.; Nishino, T.; Arasu, N. P.; Vázquez, H.; Kiguchi, M. Highly-Conducting Molecular Circuits Based on Antiaromaticity, *Nat. Commun.* **2017**, *8*, 15984.

(6) Chen, Z.; Wannere, C. S.; Corminboeuf, C.; Puchta, R.; Schleyer, P. v R. Nucleus-Independent Chemical Shifts (NICS) as an Aromaticity Criterion. *Chem. Rev.* **2005**, *105*, 3842–3888.

(7) Sundholm, D.; Fliegl, H.; Berger, R. J. F. Calculations of Magnetically Induced Current Densities: Theory and Applications, *WIREs Comput. Mol. Sci.* **2016**, *6*, 639–678.

(8) Yamashina, M.; Tanaka, Y.; Lavendomme, R.; Ronson, T. K.; Pittelkow M.; Nitschke J. R. An Antiaromatic-Walled Nanospace, *Nature* **2019**, *574*, 511–515.

(9) Pedersen, S. K.; Eriksen, K.; Karaush-Karmazin, N. N.; Minaev, B.; Ågren, H.; Baryshnikov, G. V.; Pittelkow, M. Anti-Aromatic *vs.* Induced Paratropicity: Synthesis and Interrogation of a Dihydro-Diazatrioxa[9]circulene With a Proton Placed Directly Above the Central Ring. *Angew. Chem. Int. Ed.* **2020**, *59*, 5144-5150.

(10) Baryshnikov, G. V.; Valiev, R. R.; Kuklin, A. V.; Sundholm, D.; Ågren, H. Cyclo[18]carbon: Insight into Electronic Structure, Aromaticity, and Surface Coupling. *J. Phys. Chem. Lett.* **2019**, *10*, 6701–6705.

(11) Berger, R. J. F.; Viel, A. The symmetry principle of antiaromaticity. *Zeitschrift für Naturforschung B*. **2020**, *75*, 327–339.

(12) Feixas, F.; Matito, E.; Poater, J.; Solà, M. Quantifying Aromaticity with Electron Delocalisation Measures. *Chem. Soc. Rev.* **2015**, *44*, 6434–6451.

(13) Van Vleck J. H. *The theory of electric and magnetic susceptibilities*, Oxford, Clarendon Press, 1932.

(14) Lazzeretti P. General Connections Among Nuclear Electromagnetic Shieldings and Polarizabilities. *Adv. Chem. Phys.* **1989**, *75*, 507–549.

(15) Lazzeretti, P.; Malagoli, M.; Zanasi R. Computational Approach to Molecular Magnetic Properties by Continuous Transformation of the Origin of the Current Density. *Chem. Phys. Lett.* **1994**, *220*, 299–304.

(16) Lazzeretti P. Ring Currents. *Prog. Nucl. Mag. Res. Sp.* **2000**, *36*, 1–88.

(17) Guo, R.; Uddin, M. N.; Price, L. S.; Price S. L. The Calculation of the Diamagnetic Susceptibility Tensors of Organic Crystals: from Coronene to Pharmaceutical Polymorphs. *J. Phys. Chem. A* **2020**, *124*, 1409-1420.

(18) Hegstrom, R. A.; Lipscomb, W. N. Paramagnetism in Closed-Shell Molecules. *Rev. Mod. Phys.* **1968**, *40*, 354–358.

(19) Fowler, P. W.; Steiner, E. Paramagnetic Closed-Shell Molecules: the Isoelectronic series CH^+, BH and BeH^-. *Mol. Phys.* **1991**, *74*, 1147–1158.

(20) Sauer, S. P. A.; Enevoldsen, T.; Oddershede, J. Paramagnetism of Closed Shell Diatomic Hydrides with Six Valence Electrons. *J. Chem. Phys.* **1993**, *98*, 9748–9757.

(21) Ruud, K.; Helgaker, T.; Bak, K. L.; Jørgensen, P.; Olsen, J. Accurate Magnetizabilities of the Isoelectronic Series BeH^-, BH, and CH^+. The MCSCF-GIAO Approach. *Chem. Phys.* **1995**, *195*, 157–169.

(22) Carrington, A. The Temperature-Independent Paramagnetism of Permanganate and Related Complexes, Mol. Phys. **1960**, *3*, 271–275.

(23) Peeks, M. D.; Claridge, T. D. W.; Anderson, H. L. Aromatic and Antiaromatic Ring Currents in a Molecular Nanoring. *Nature*, **2017**, *541*, 200–203.

(24) Valiev, R. R.; Fliegl, H.; Sundholm, D. Closed-shell paramagnetic porphyrinoids. *Chem. Commun.* **2017**, *53*, 9866–9869.

(25) Valiev, R. R.; Fliegl, H.; Sundholm D. Optical and magnetic properties of antiaromatic porphyrinoids. *Phys. Chem. Chem. Phys.* **2017**, *19*, 25979–25988.

(26) Valiev, R. R.; Baryshnikov, G. V.; Sundholm, D.; Relations Between the Aromaticity and Magnetic Dipole Transitions in the Electronic Spectra of Hetero[8]circulenes, *Phys. Chem. Chem. Phys.* **2018**, *20*, 30239–30246.

(27) Helgaker, T.; Coriani, S.; Jørgensen, P.; Kristensen, K.; Olsen, J.; Ruud, K. Recent Advances in Wave Function-Based Methods of Molecular-Property Calculations, *Chem. Rev.* **2012**, *112*, 543-631.

(28) Ruud, K.; Helgaker, T.; Bak, K. L.; Jørgensen, P.; Jensen, H. J. Aa. Hartree–Fock limit Magnetizabilities from London Orbitals, *J. Chem. Phys.* **1993**, *99*, 3847-3859.

(29) Ruud, K.; Skaane, H.; Helgaker, T.; Bak, K. L.; Jørgensen, P. Magnetizability of Hydrocarbons. *J. Am. Chem. Soc.* **1994**, *116*, 10135-10140.

(30) Dahle, P.; Ruud, K.; Helgaker, T.; Taylor P. R. Molecular Polarizabilities and Magnetizabilities. *Theor. Comp. Chem.* **1999**, *6*, 147-188.

(31) Stevens, R. M.; Pitzer, R. M.; Lipscomb, W. N. Perturbed Hartree—Fock Calculations. I. Magnetic Susceptibility and Shielding in the LiH Molecule. *J. Chem. Phys.* **1963**, *38*, 550-560.

(32) Pascal, P. Recherches Magnetochimiques. *Ann. Chim. Phys*. **1910**, *19*, 5-70.

(33) Zhao, Y.; Truhlar, D. G. The M06 Suite of Density Functionals for Main Group Thermochemistry, Thermochemical Kinetics, Noncovalent Interactions, Excited States, and Transition Elements: Two New Functionals and Systematic Testing of Four M06-class Functionals and 12 other Functionals. *Theor. Chem. Acc.* **2008**, *120*, 215–241

(34) Weigend, F.; Ahlrichs, R. Balanced Basis Sets of Split Valence, Triple Zeta Valence and Quadruple Zeta Valence Quality for H to Rn: Design and Assessment of Accuracy. *Phys. Chem. Chem. Phys.* **2005**, *7*, 3297–3305

(35) Baryshnikov, G. V.; Valiev, R. R.; Lie, Q.; Lie, C.; Xie, Y.; Ågren, H. Computational Study of Aromaticity, ^{1}H NMR Spectra and Intermolecular Interactions of Twisted Thianorhexaphyrin and Its Multiply Annulated Polypyrrolic Derivatives. *Phys. Chem. Chem. Phys.* **2019**, *21*, 25334-25343.

(36) Valiev, R. R.; Fliegl, H.; Sundholm, D. Bicycloaromaticity and Baird-type bicycloaromaticity of dithienothiophene-bridged [34] octaphyrins. *Phys. Chem. Chem. Phys.* **2018**, *20*, 17705-17713.

(37) Wolinski, K.; Hilton J. F.; Pulay, P. Efficient Implementation of the Gauge-Independent Atomic Orbital Method for NMR Chemical Shift Calculations. *J. Am. Chem. Soc.* **1990**, *112*, 8251-8260.

(38) Fisch, M. J.; Trucks, G. W.; Schlegel, H. B.; Scuseria, G. E.; Robb, M. A.; Cheeseman, J. R.; Scalmani, G.; Barone, V.; Petersson, G. A.; Nakatsuji, H.; et al. *Gaussian 16, Revision A.03*, Gaussian, Inc.,Wallingford CT, **2016**.

(39) Jusélius, J.; Sundholm, D. Calculation of Current Densities Using Gauge-Including Atomic Orbitals. *J. Chem. Phys.* **2004**. *121*, 3952-3963.

(40) Gauge-Including Magnetically Induced Currents (GIMIC) program is distributed on GitHub platform and can be downloaded through the link: https://github.com/qmcurrents/gimic.

(41) Granovsky, A. A. Firefly version 8.0.0, http://classic.chem.msu.su/gran/firefly/index.html.

(42) Valiev, R. R.; Benkyi, I.; Konyshev, Y. V.; Fliegl, H.; Sundholm, D. Computational Studies of Aromatic and Photophysical Properties of Expanded Porphyrins. *J. Phys. Chem. A* **2018**, *122*, 4756−4767.

(43) Herges, R. Topology in Chemistry: Designing Möbius Molecules. *Chem. Rev.* **2006**, *106*, 4820-4842.

(44) Kaiser, K.; Scriven, L. M.; Schulz, F.; Gawel, P.; Gross, L.; Anderson, H. L. An Sp-Hybridized Molecular Carbon Allotrope, Cyclo[18]Carbon. *Science.* **2019**, *365* (6459), 1299–1301.

(45) Fowler, P. W.; Mizoguchi, N.; Bean, D. E.; Havenith, R. W. A. Double Aromaticity and Ring Currents in All-Carbon Rings. *Chem. - A Eur. J.* **2009**, *15*, 6964–6972.

(46) Baryshnikov, G. V.; Valiev, R. R.; Kuklin, A. V.; Sundholm, D.; Ågren H. Cyclo[18]carbon: Insight into Electronic Structure, Aromaticity, and Surface Coupling. *J. Phys. Chem. Lett.* **2019**, *10* (21), 6701–6705.

(47) Fliegl, H.; Sundholm, D. Aromatic Pathways of Porphins, Chlorins, and Bacteriochlorins. *J. Org. Chem.* **2012**, *77*, 3408–3414.

(48) Valiev, R. R.; Fliegl, H.; Sundholm, D. Insights into Magnetically Induced Current Pathways and Optical Properties of Isophlorins. *J. Phys. Chem. A*, **2013**, *117*, 9062–9068.

(49) Fliegl, H.; Tauber, S.; Lehtonen, O.; Sundholm D. The Gauge Including Magnetically Induced Current Method. *Phys. Chem. Chem. Phys.* **2011**, *13*, 20500–20518.

(50) Tsuda, A.; Osuka, A. Fully Conjugated Porphyrin Tapes with Electronic Absorption Bands That Reach into Infrared. *Science* **2001**, *293*, 79–82.

(51) Ikeda, T.; Aratani, N.; Osuka, A. Synthesis of Extremely π-Extended Porphyrin Tapes from Hybrid meso-meso Linked Porphyrin Arrays: An Approach Towards the Conjugation Length. *Chemistry–An Asian Journal*. **2009**, *4*, 1248–1256.

(52) Nakamura, Y.; Aratani, N.; Furukawa, K.; Osuka, A. Synthesis and Characterizations of Free Base and Cu(II) Complex of a Porphyrin Sheet. *Tetrahedron* **2008**, *64*, 11433–11439.

(53) Tanaka, T.; Osuka A. Conjugated Porphyrin Arrays: Synthesis, Properties and Applications for Functional Materials, *Chem. Soc. Rev.* **2015**, *44*, 943–969.

(54) Baryshnikov, G. V.; Valiev, R. R.; Karaush, N. N.; Minaev, B. F. Aromaticity of the Planar Hetero[8]circulenes and Their Doubly Charged Ions: NICS and GIMIC Characterization. *Phys. Chem. Chem. Phys.* **2014**, *16*, 15367–15374.

(55) Baryshnikov, G. V.; Valiev, R. R.; Karaush, N. N.; Sundholm, D.; Minaev, B. F. Aromaticity of the Doubly Charged [8]Circulenes. *Phys. Chem. Chem. Phys.* **2016**, *18*, 8980–8992.

(56) Baryshnikov, G. V.; Valiev, R. R.; Cherepanov, V. N.; Karaush-Karmazin, N. N.; Minaeva, V. A.; Minaev, B. F.; Ågren, H. Aromaticity and Photophysics of Tetrasila- and Tetragerma-Annelated Tetrathienylenes as New Representatives of the Hetero[8]circulene Family. *Phys. Chem. Chem. Phys.* **2019**, *21*, 9246–9254.

(57) Nakamura, Y.; Aratani, N.; Shinokubo, H.; Takagi, A.; Kawai, T.; Matsumoto, T.; Yoon, Z. S.; Kim, D. Y.; Ahn, T. K.; Kim, D.; Muranaka, A.; Kobayashi, N.; Osuka A. A Directly Fused Tetrameric Porphyrin Sheet and Its Anomalous Electronic Properties That Arise from the Planar Cyclooctatetraene Core. *J. Am. Chem. Soc.* **2006**, *128*, 4119–4127.

(58) Nakamura, Y.; Aratani, N.; Osuka, A. Experimental and Theoretical Investigations into the Paratropic Ring Current of a Porphyrin Sheet. *Chem. Asian J.* **2007**, *2*, 860–866.

(59) Woodward, R. B. Totalsynthese des Chlorophylls. *Angew. Chem*., **1960**, *72*, 651–662.

(60) Reddy, J. S.; Anand, V. G. Planar Meso Pentafluorophenyl Core Modified Isophlorins. *J. Am. Chem. Soc*., **2008**, *130*, 3718–3719.

(61) Reddy, B. K.; Basavarajappa, A.; Ambhore, M. D.; Anand V. G. Isophlorinoids: The Antiaromatic Congeners of Porphyrinoids. *Chem. Rev.,* **2017**, *117*, 3420–3443;

(62) Chatterjee, T.; Srinivasan, A.; Ravikanth, M.; Chandrashekar, T. K. Smaragdyrins and Sapphyrins Analogues. *Chem. Rev*., **2017**, *117*, 3254–3328.

(63) Reddy, J. S.; Mandal, S.; Anand, V. G. Cyclic Oligofurans: One-Pot Synthesis of 30π and 40π Expanded Porphyrinoids. *Organic letters*, **2006**, *8*, 5541-5543.

(64) Glick, R. E. On The Diamagnetic Susceptibility of Gases *J. Phys. Chem.* **1961**, *65*, 1552–1555.

(65) Jasat, A.; Dolphin, D. Expanded Porphyrins and Their Heterologs. *Chem. Rev.* **1997**, *97*, 2267-2340.

(66) Cha, W. Y.; Soya, T.; Tanaka, T.; Mori, H.; Hong, Y.; Lee, S.; Park, K. H.; Osuka, A.; Kim, D. Multifaceted [36]octaphyrin (1.1.1.1.1.1.1.1): deprotonation-induced switching among nonaromatic, Möbius aromatic, and Hückel antiaromatic species. *Chem. Commun.* **2016**, *52*, 6076-6078.